Direct Electromagnetic Acceleration of a Compact Toroid to High Density and High Speed

Robert E. Peterkin, Jr.*
High Energy Plasma Division, Phillips Laboratory, Kirtland Air Force Base, Kirtland, New Mexico 87117
(Received 12 April 1994)

The direct acceleration and compression of a magnetically confined plasma, called a compact toroid (CT), by an electrical discharge are investigated with numerical time-dependent magnetohydrodynamic computer simulations. We find that a critical dimensionless parameter P characterizes the resiliency of a CT to an acceleration over a characteristic distance, and that a CT can be compressed self-similarly and accelerated to an arbitrary nonrelativistic speed when P is maintained in an appropriate range.

PACS numbers: 52.55.Hc, 52.30.–q, 52.65.Kj, 52.75.Di

There are a variety of devices for accelerating a macroscopic quantity of mass to high speed including light gas guns, electromagnetic rail guns, and deflagration guns. It has been previously conjectured that a magnetically confined ring could, in principal, be accelerated to high speed by a sufficiently energetic pulsed electrical discharge [1]. For many possible applications, high mass and high speed are desired. There are now a number of megajoule-level pulsed power facilities throughout the world, and with these facilities comes the potential for imparting speeds of $\sim 10^6$ m/s to milligram masses. Megajoule-level plasma experiments are expensive, and the plasmas produced in the laboratory are often difficult to control. Therefore, detailed computer simulation of plasma dynamics is of great value in increasing the understanding and decreasing the costs of proposed plasma experiments [2]. If done carefully, numerical simulation can lead to a better theoretical understanding of possibly complex behavior.

A compact toroid (CT) is an axisymmetric toroidal plasma with a helical magnetic field structure [3]. When formed between two coaxial electrodes, a CT can be accelerated by an electrical discharge and the CT behaves like a plasma armature in a coaxial railgun. A CT, moving at hypervelocity ($>10^5$ m/s), may have a variety of uses [1], including a very fast opening switch [4], the production of keV x rays upon stagnation at a wall [5,6], and the initiation of fusion reactions during the collision of a CT with another object [1], which may even be a second CT. These applications of compact toroids involve physical processes that are enhanced at high plasma density. Therefore, a design that compresses the CT as it is accelerated is of interest. This Letter gives a prescription for how to accelerate a CT from rest to an arbitrary nonrelativistic speed between a pair of converging electrodes, by introducing a critical dimensionless parameter, P, that describes the resiliency of a CT to an accelerating force. The acceleration of a CT from rest to high speed has been studied for a variety of configurations and values of P via two-dimensional, axisymmetric, time-dependent, magnetohydrodynamic (MHD) computer simulations with the arbitrary coordinate code, MACH2 [7]. The approximation of axisymmetry is valid for CT rings because they are stable against tilting [8].

A localized parcel of plasma to which an accelerating force is applied is, in general, unstable to fluid instabilities of the Rayleigh-Taylor variety [9,10]. Such instabilities effectively limit the time over which an accelerating force can be applied before the parcel is disrupted. However, because a CT has a small plasma β and is in a minimum energy state with nonzero magnetic helicity [11], it is less likely to disrupt when accelerated.

In the MARAUDER effort at the Phillips Laboratory, described in detail by Degnan *et al.* [12], a CT is formed in a magnetized plasma gun with the first of two pulsed electrical discharges. The second discharge is applied across the upstream end of the CT which creates a $\mathbf{J} \times \mathbf{B}$ force on the plasma that accelerates it. Simulation has been used to guide the design of these experiments, and there is quantitative agreement between theory, simulation, and experiment.

The cross section for a particular converging electrode geometry with a radial convergence factor of 10 is illustrated in Fig. 1. This geometry is chosen to allow direct drive of the CT to high speed by an external energy source. (An alternate idea that relies on inductive energy storage employs a pair of compound cones and is not discussed here.) The CT formation gun and trapping volume would be at the lower (upstream) end of the figure. The conical electrode geometry is self-similar: The ratio of the electrode gap to the radius is a constant along a line that bisects the interelectrode gap. A CT that undergoes self-similar compression maintains a constant aspect ratio; therefore the length of the CT, ℓ_{CT}, contracts in proportion to the decrease in the electrode gap during compression, and the mass density increases.

A simple model for CT dynamics between a pair of conical electrodes treats the CT as a point object that is characterized by its mass m and its magnetic energy U_B. The cones are characterized by a pair of angles, θ_1 and θ_2, measured from the symmetry axis. (For the geometry of Fig. 1, $\theta_1 = 25.25°$ and $\theta_2 = 33.17°$.) At a time t the magnetic O point of the CT is located at the position $r(t)$, where r is the spherical polar radius from the apex of the cones. In the absence of resistive decay, magnetic flux is conserved. In this case, the magnetic energy of a CT that undergoes self-similar compression scales inversely with r:

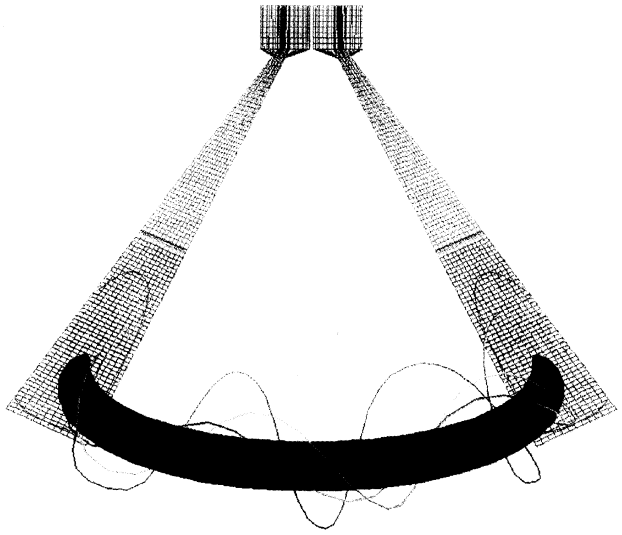

FIG. 1. Sample initial mass density and magnetic field structure are superimposed on an outline of the computational mesh of a MACH2 numerical simulation of CT compression and acceleration. Here, $r_0 = 1$ m and $\ell_{CT}(t = 0) \approx 30$ cm. Three magnetic field lines from the initial Taylor state are shown to twist around a mass density isosurface. Lines with a higher (lower) ratio of azimuthal to poloidal components are red (blue).

$U_B = U_{B0}\, r_0/r$, where U_{B0} is the magnetic energy at some initial position r_0. The converging cones exert a force on the CT, $\mathbf{F}_{\text{cone}} = -\nabla U_B$, that is directed outward in the $+\hat{\mathbf{r}}$ direction. It is necessary to overcome this force if a CT is to be compressed to smaller radius. One possible mechanism is to apply an electrical discharge upstream of the CT so an electrical current $i(t)$ flows in the plasma between the electrodes. Such a discharge acts like a piston behind the CT and applies a force in the $-\mathbf{r}$ direction: $\mathbf{F}_{\text{compress}} = -\frac{1}{2}L'i(t)^2\hat{\mathbf{r}}$. $L' = (\mu_0/2\pi)\ln[\tan(\theta_2/2)/\tan(\theta_1/2)]$ is the inductance per unit length of nested cones ($L' = 57$ nH/m for the geometry of Fig. 1) and μ_0 is the vacuum permeability. The radial force on the low β CT is [13]

$$F_r = \frac{r_0\, U_{B0}}{r^2} - \frac{L'i(t)^2}{2}. \tag{1}$$

Written in terms of the dimensionless variable, $y(t) \equiv r(t)/r_0$, Eq. (1) has the form

$$\ddot{y}(t) - \omega_0^2 y(t)^{-2} + \Omega(t)^2 = 0, \tag{2}$$

where $\omega_0^2 = U_{B0}/mr_0^2$ and $\Omega(t)^2 = L'i(t)^2/2mr_0$.

Of course, in reality a CT is not a point object and the dynamics when under the influence of a piston current may not obey the simple form of Eq. (2). A measure of the stiffness of a CT is its mean Alfvén speed, defined via $\frac{1}{2}m\overline{v_A^2} = U_B$. In order to achieve self-similar compression of a real CT of finite $\overline{v_A^2}$, the acceleration must be constrained so that the change in the CT speed is not significantly greater than $(\overline{v_A^2})^{1/2}$ during an Alfvén transit time across ℓ_{CT}. Therefore

$$\int (\ddot{r})dt \lesssim (\overline{v_A^2})^{1/2}, \tag{3}$$

where $dt = d\ell_{CT}/(\overline{v_A^2})^{1/2}$. For a point object, the acceleration is constant over ℓ_{CT}. As a consequence, Eq. (3) can be written as

$$P[r(t)] \equiv \left| \frac{m\ddot{r}\ell_{CT}}{2U_B} \right| \lesssim 1, \tag{4}$$

where the dimensionless parameter P is similar to κ_{eff} of Ref. [13]. If P is too small, however, the CT can be made to oscillate by the piston force. The oscillation frequency about an average trajectory $\bar{r}$ is $(2U_B/m\bar{r}^2)^{1/2}$ [13]. Oscillations will not have time to develop if the product of the bounce frequency with the acceleration time is less than unity. For constant $\ddot{r}$, the acceleration time over a distance r_0 is $(2r_0/\ddot{r})^{1/2}$. In terms of P, the condition for self-similar compression without oscillations is then

$$\frac{2\ell_{CT}r_0}{\bar{r}^2} \lesssim P \lesssim 1. \tag{5}$$

It is found from simulation that the degree to which a CT obeys the simple point model described by Eq. (2) is indeed determined by the dimensionless ratio P. Interestingly, when written in terms of the mean Alfvén speed, P resembles the inverse of the Froude number from fluid mechanics [14]. For a CT undergoing constant acceleration, P scales as r^2, and has a maximum value P_0 at $t = 0$.

In general, a self-consistent solution to Eq. (2) requires a dynamical model for $i(t)$ which may involve $y(t)$. It is straightforward to solve Eq. (2), usually via numerical integration, for various $i(t)$. In lieu of solving Eq. (2), however, it is interesting to ask what current wave form is required to achieve a particular desirable acceleration. For example, the equilibrium value, $i_{\text{eq}} = (2U_B/r\,L')^{1/2}$, will maintain the CT at zero acceleration. The piston current must exceed this value for the CT to be driven downstream to smaller radius (smaller y).

A simple way for a CT that is initially at rest in the laboratory frame to achieve high speed is to apply a constant acceleration so that $\ddot{y}(t) = -g/r_0, \forall t$; then the point CT trajectory is $r(t) = r_0 - \frac{1}{2}gt^2$ with $\dot{r} = -gt$. A radial convergence factor f, $y_f = 1/f$, will occur at a time t_f when the radial speed is v_f : $t_f = 2r_0(1 - y_f)/v_f$. In terms of y_f and v_f, the constant acceleration trajectory is

$$y(t) \equiv \frac{r(t)}{r_0} = 1 - \frac{1}{1 - y_f}\left(\frac{tv_f}{2r_0}\right)^2. \tag{6}$$

The piston current that will accelerate a point CT from rest at r_0 to a final speed v_f at r_0/f is

$$i[y(t)]^2 = \frac{1}{r_0L'}\left(\frac{2U_{B0}}{y(t)^2} + \frac{mv_f^2}{1 - y_f}\right). \tag{7}$$

This current has its minimum value at $t = 0$ and rises monotonically with a positive second derivative.

A family of numerical simulations in the geometry of Fig. 1 was performed with current wave forms described by Eq. (7), where $y_f = 1/10$ and $v_f = 2.0 \times 10^5$ m/s is achieved after 8.24 μs. Initially, the simulations begin with a plasma in a Taylor state [11] at the upstream volume between the compression cones of Fig. 1. The mass is also initially distributed so that density isocontours lie on poloidal magnetic flux lines with the maximum density at the magnetic O point and fall monotonically to a minimum value at the separatrix of the CT. Sample initial magnetic and mass density structures for the time-dependent simulations are illustrated in Fig. 1. To ease comparison between the simulations and the point model, the simulations assume a perfectly conducting plasma, and the rotation that is induced by the interaction of the piston current with the CT is suppressed. The trajectories obtained from simulation for three different values of P_0 are shown superimposed on the point model trajectory of Eq. (6) in Fig. 2. The trajectory for the simulated acceleration of a CT is defined by the location of the magnetic O point which is close to the location of the center of mass.

The case of $P_0 = 0.025$ is illustrative of all cases in which $P_0 \ll 2\ell_{CT} r_0/\bar{r}^2$. This simulation shows a bounce at the expected frequency $\sim\sqrt{2}\,\omega_0$. The case of $P_0 = 25$ is illustrative of all cases in which $P \gg 1$, whereupon the piston current pushes the CT to the outer electrode causing the CT to lose contact with the inner electrode. This behavior is called "blowby" in Ref. [13]. The simulated trajectory for such cases shows an acceleration phase at early times, followed by a constant speed phase after blowby occurs and the piston current ceases to perform useful work on the CT. The preferred behavior occurs when P is within the approximate range of Eq. (5). In such cases, the trajectory is close to that predicted by the point model. The $P_0 = 1.25$ trajectory is shown in Fig. 2.

Numerical simulations from different initial conditions that all have the same values of P behave similarly. For example, Fig. 3 shows three simulated trajectories each of which has $P_0 = 1.25$. It is important to note that the initial distribution of mass in the CT is not crucial. The piston current wave form that was chosen to accelerate a low mass (0.5 mg), low initial magnetic energy (2.22 kJ) CT is also shown in Fig. 3.

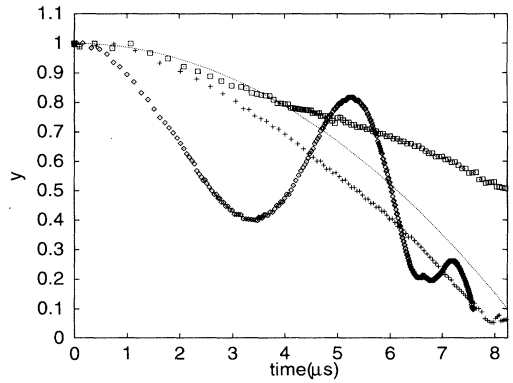

FIG. 2. Trajectories for simulated CT compression and acceleration compared to the point trajectory of Eq. (2). $P_0 = 0.025$ (diamonds), $P_0 = 1.25$ (plus signs), $P_0 = 25$ (boxes), and point model (dashed line).

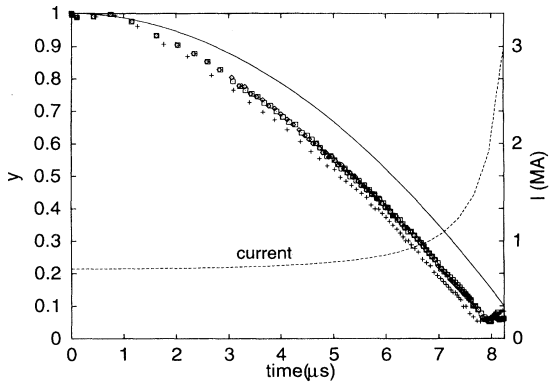

FIG. 3. Trajectories from numerical simulation of the $P_0 = 1.25$ case with three different sets of initial conditions: high mass (5 mg), high initial magnetic energy (22.2 kJ) (diamonds); low mass (0.5 mg), low initial magnetic energy (2.22 kJ) (plus signs); and high mass, initially uniform mass density, high initial magnetic energy (boxes). The point model trajectory is shown for reference (dashed line). Also shown is the piston current wave form for the low mass, low initial magnetic energy case.

This model gives guidance for how to impart to a CT any nonrelativistic speed. For example, if 1.0×10^6 m/s is desired in the geometry of Fig. 1, the acceleration time is 1.65 μs at constant acceleration. If this time is too short for practical reasons, a different geometry can be used to lengthen the time that is required to achieve a particular final speed. Figure 4 shows an overlay of a mass density and magnetic field lines from a simulated CT with $P_0 \sim 1$ at $t = 0$, 3.0, and 6.0 μs into a constant acceleration discharge in a self-similar converging 8° pair of cones ($L' = 67$ nH/m) that are designed to achieve 1.0×10^6 m/s after 6.5 μs. Because P is in the proper domain for a robust compression and acceleration, the desired final speed and compression ratio $f = 10$ is achieved. For this simulation, the CT mass and initial magnetic energy are chosen to be 2 mg and 100 kJ, respectively. As a consequence, the initial acceleration current is 3.2 MA and it rises to a peak value of 9.6 MA. Currents and energies of this order are now, or will soon become, available at a variety of pulsed power laboratories throughout the world. Based on our simulations, we conjecture that any nonrelativistic speed can be achieved in the laboratory by a macroscopic ring that is driven by a sufficiently energetic source as long as P is maintained in the preferred range of Eq. (5) during the entire acceleration time.

An obvious question is how to achieve a current wave form of the type described by Eq. (7). Such a wave

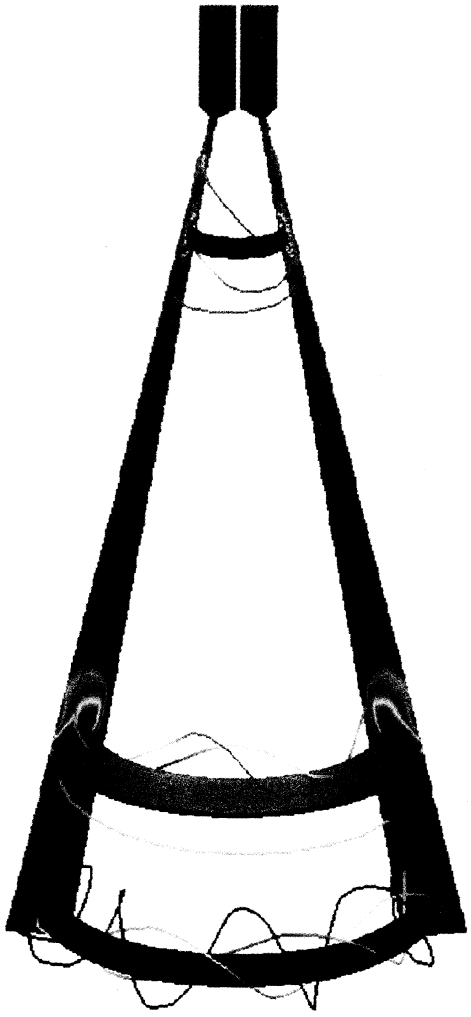

FIG. 4. Superposition of snapshots of the mass density and magnetic field lines of a CT at $t = 0$, 3.0 and 6.0 μs in a long converging geometry that is designed to achieve a final speed of 10^6 m/s in 6.5 μs. Three magnetic field lines from the initial toroid are shown to twist around a mass density isosurface (blue). The later-time data each have an almost purely azimuthal field line located upstream of the CT that represents the piston field. The mass density increases with time (red is higher density than blue).

form can be approximated by an explosive magnetic generator [15]. Numerical simulations of CT compression and acceleration with explosive flux compression current wave forms show similar behavior to those simulations discussed herein.

The author has enjoyed fruitful discussions with C. W. Hartman, R. J. Leiweke, N. F. Roderick, U. Shumlak, and P. J. Turchi. We also acknowledge the use of the Cray Research C916/16512 supercomputer at the Army Corps of Engineers Waterways Experiment Station in Vicksburg, MS. This work was partially supported by the Air Force Office of Scientific Research.

*Electronic address: bob@ppws07.plk.af.mil

[1] C. W. Hartman and J. H. Hammer, Phys. Rev. Lett. **48**, 929 (1982).
[2] See, e.g., J. M. Dawson, V. Decyk, R. Sydora, and P. Liewer, Phys. Today **46**, No. 3, 64 (1993).
[3] H. Alfvèn, in *Proceedings of the Second United Nations International Conference on the Peaceful Uses of Atomic Energy, Geneva, Switzerland, 1958* (United Nations, Geneva, 1958), Vol. 31, p. 3.
[4] R. E. Peterkin, Jr., J. H. Degnan, T. W. Hussey, N. F. Roderick, and P. J. Turchi, IEEE Trans. Plasma Sci. **21**, 522 (1993).
[5] M. Gee, P. Nowak, and G. Zimmerman, Technical Report UCRL-53951, Lawrence Livermore National Laboratory, Livermore, CA 94551, 1989.
[6] M. R. Douglas, R. E. Peterkin, Jr., T. W. Hussey, D. E. Bell, and N. F. Roderick, in *Proceedings of the Ninth International Conference on High-Power Particle Beams, Washington D.C., 1992,* edited by D. Mosher and G. Cooperstein (National Technical Information Service Report No. NTIS PB92-206168, 1992), p. 2062.
[7] M. H. Frese, R. E. Peterkin, Jr., and A. J. Giancola "MACH2: A Multiblock Two-Dimensional Magnetohydrodynamic Simulation Code" (to be published).
[8] S. Iizuka, Y. Minamitani, H. Tanaca, and Y. Kiwamoto, Phys. Rev. Lett. **53**, 918 (1984).
[9] Lord Rayleigh, *Scientific Papers* (Cambridge University Press, Cambridge, England, 1990), Vol. II, p. 200.
[10] S. Chandrasekhar, *Hydrodynamic and Hydromagnetic Stability* (Dover, New York, 1981).
[11] J. B. Taylor, Phys. Rev. Lett. **33**, 1139 (1974).
[12] J. H. Degnan *et al.,* Phys. Fluids B **5**, 2938 (1993).
[13] C. W. Hartman and J. H. Hammer, Lawrence Livermore National Laboratory Report No. LLL-Prop-191, 1984. The point model is discussed in Appendix G.
[14] L. D. Landau and E. M. Lifshitz, Fluid Mechanics (Pergamon Press, Oxford, 1959), p. 63.
[15] V. K. Chernyshev *et al.,* in *Digest of Technical Papers: Eighth IEEE International Pulsed Power Conference, San Diego, CA, 1991,* edited by R. White and K. Prestwich (The Institute of Electrical and Electronics Engineers, Inc., New York, 1991), p. 419.

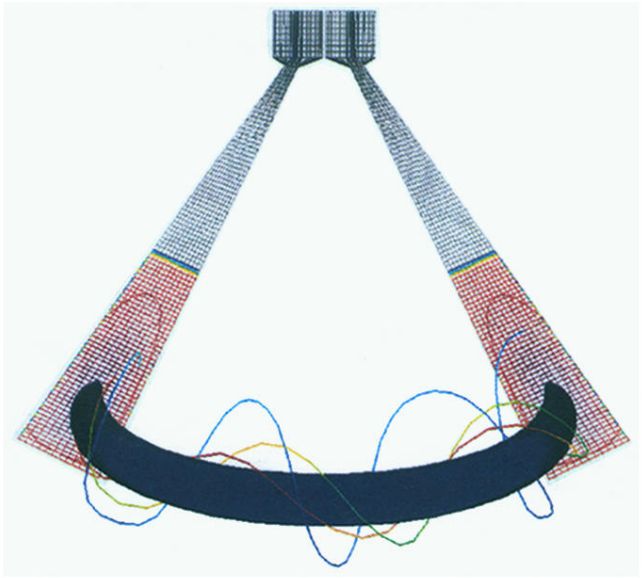

FIG. 1. Sample initial mass density and magnetic field structure are superimposed on an outline of the computational mesh of a MACH2 numerical simulation of CT compression and acceleration. Here, $r_0 = 1$ m and $\ell_{CT}(t = 0) \approx 30$ cm. Three magnetic field lines from the initial Taylor state are shown to twist around a mass density isosurface. Lines with a higher (lower) ratio of azimuthal to poloidal components are red (blue).

FIG. 4. Superposition of snapshots of the mass density and magnetic field lines of a CT at $t = 0$, 3.0 and 6.0 μs in a long converging geometry that is designed to achieve a final speed of 10^6 m/s in 6.5 μs. Three magnetic field lines from the initial toroid are shown to twist around a mass density isosurface (blue). The later-time data each have an almost purely azimuthal field line located upstream of the CT that represents the piston field. The mass density increases with time (red is higher density than blue).